

This article is published as part of the *Dalton Transactions* themed issue entitled:

Computational Chemistry of Molecular Inorganic Systems

Guest Editor: Professor Stuart MacGregor
Heriot-Watt University, Edinburgh, U.K.

Published in [issue 42, 2011](#) of *Dalton Transactions*

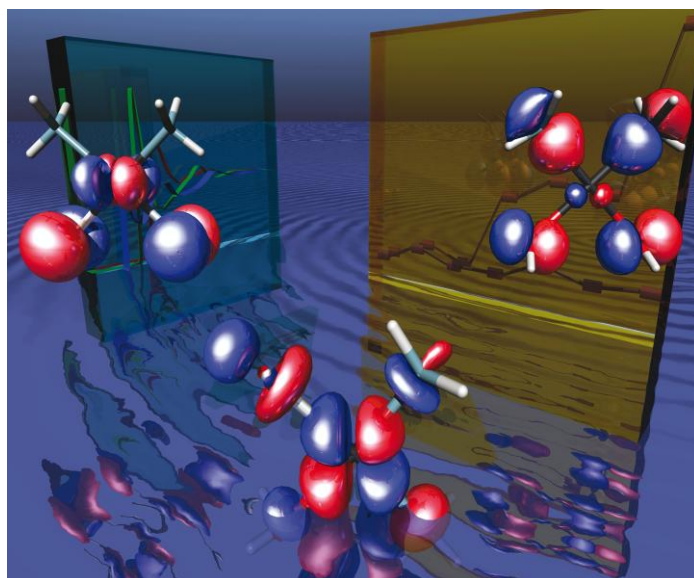


Image reproduced with the permission of Hirofumi Sato

Articles in the issue include:

COMMUNICATION:

[Comparison of different ruthenium–alkylidene bonds in the activation step with N-heterocyclic carbene Ru-catalysts for olefins metathesis](#)

Albert Poater, Francesco Ragone, Andrea Correa and Luigi Cavallo
Dalton Trans., 2011, DOI: 10.1039/C1DT10959F

HOT ARTICLES:

[Matrix infrared spectroscopic and density functional theoretical investigations on thorium and uranium atom reactions with dimethyl ether](#)

Yu Gong and Lester Andrews
Dalton Trans., 2011, DOI: 10.1039/C1DT10725A

[Reductive coupling of carbon monoxide by U\(III\) complexes—a computational study](#)

Georgina Aitken, Nilay Hazari, Alistair S. P. Frey, F. Geoffrey N. Cloke, O. Summerscales and Jennifer C. Green
Dalton Trans., 2011, DOI: 10.1039/C1DT10692A

[Prediction of high-valent iron K-edge absorption spectra by time-dependent Density Functional Theory](#)

P. Chandrasekaran, S. Chantal E. Stieber, Terrence J. Collins, Lawrence Que, Jr., Frank Neese and Serena DeBeer
Dalton Trans., 2011, DOI: 10.1039/C1DT11331C

Visit the *Dalton Transactions* website for more cutting-edge inorganic and organometallic research
www.rsc.org/dalton

Cite this: *Dalton Trans.*, 2011, **40**, 11095

www.rsc.org/dalton

PAPER

Theoretical study on intramolecular allene-diene cycloadditions catalyzed by PtCl₂ and Au(I) complexes†

Sergi Montserrat,^a Isaac Alonso,^b Fernando López,^{*c} José L. Mascareñas,^{*b} Agustí Lledós^{*a} and Gregori Ujaque^{*a}

Received 6th June 2011, Accepted 12th August 2011

DOI: 10.1039/c1dt11061f

The intramolecular [4C+3C] cycloaddition reaction of allenedienes catalysed by PtCl₂ and several Au(I) complexes has been studied by means of DFT calculations. Overall, the reaction mechanism comprises three main steps: (i) the formation of a metal allyl cation intermediate, (ii) a [4C(4π)+3C(2π)] cycloaddition that produces a seven-membered ring and (iii) a 1,2-hydrogen migration process on these intermediates. The reaction proceeds with complete diastereochemical control resulting from a favoured *exo*-like cycloaddition. Allene substituents have a critical influence in the reaction outcome and mechanism. The experimental observation of [4C+2C] cycloadducts in the reaction of substrates lacking substituents at the allene terminus can be explained through a mechanism involving Pt(IV)-metallacycles. With gold catalysts it is also possible to obtain [4C+2C] cycloaddition products, but only with substrates featuring terminally disubstituted allenes, and employing π-acceptor ligands at gold. However the mechanism for the formation of these adducts is completely different to that proposed with PtCl₂, and consists of the formation of a metal allyl cation, subsequent [4C+3C] cycloaddition and a 1,2-alkyl shift (ring contraction). Electronic analysis indicates that the divergent pathways are mainly controlled by the electronic properties of the gold heptacyclic species (L-Au-C₂), in particular, the backdonation capacity of the metal center to the unoccupied C₂ (*pπ*-orbital) of the intermediate resulting from the [4C+3C] cycloaddition. The less backdonation, (*i.e.* using P(OR)₃Au⁺ complexes), the more favoured is the 1,2-alkyl shift.

Introduction

Cycloaddition reactions allow the formation of cyclic systems from acyclic reactants, and usually involve the rearrangement of π-electrons.¹ Although direct cycloadditions to form cycles of four, five or six members are relatively common, seven-membered cycles are much less accessible.² One of the most interesting approaches to these cycles involves the combination of a diene and an allyl cation, a component that contributes 3-centers and two π-electrons.³ A critical step for the success of these [4C+3C] cycloadditions is the *in situ* formation of an appropriate allyl cation moiety.

It is well known that platinum and gold complexes can activate C–C multiple bonds to generate several types of reactive intermediates that evolve into different types of products.⁴ Mechanistic studies on these transformations are very scarce, especially in the case of gold, mainly because of the difficulties for isolating intermediates.⁵ Thus, theoretical studies represent an important tool to gain insights on these reaction mechanisms.^{6,7}

In 2007, two different groups independently described a platinum- and a gold-catalysed synthesis of cyclopentadienes from vinyl allenes, and suggested that the reactions involve the activation of the allene to make a metal-pentadienyl cation intermediate.^{8,9} We then envisioned the possibility of using simple allenes as precursors of related metal allyl cations, so they could participate as 3-carbon atom components in the [4C+3C] cycloaddition reactions to dienes.^{10,11} Indeed, new intramolecular [4C+3C] cycloaddition reactions of allenedienes catalysed by platinum and gold complexes were subsequently developed.¹² The reactions proceed with complete diastereochemical control and provide a variety of interesting bicyclic products featuring seven-membered rings. Some representative substrates used in these reactions catalyzed by PtCl₂ are presented in Table 1.¹²

On the basis of several theoretical and experimental data, a general reaction mechanistic pathway has been recently proposed

^aDepartament de Química, Universitat Autònoma de Barcelona, 08193, Cerdanyola del Vallès, Spain. E-mail: agusti@klingon.uab.es; Fax: +34-935812920; Tel: +34-935811716

^bDepartamento de Química Orgánica, Centro Singular de Investigación en Química Biológica y Materiales Moleculares, y Unidad Asociada al CSIC, Universidad de Santiago de Compostela, 15782, Santiago de Compostela, Spain

^cInstituto de Química Orgánica General (CSIC), Juan de la Cierva 3, 28006, Madrid, Spain

† Electronic supplementary information (ESI) available: Table of electronic NBO and Bader analysis of the seven membered intermediates **3** and **3'**. Absolute energies (in hartrees) and cartesian coordinates of the optimized structures. See DOI: 10.1039/c1dt11061f

Table 1 General scheme for the reaction catalysed by PtCl₂¹²

Entry	Substrate	Product	Yield
1			92 ^a
2			62 ^b
3			23 ^c
4			95

4D:4D'
(6:4)

X = C(CO₂Et)₂; R₁, R₂ = H, CH₃, Ph.^a Reaction catalysed by 10% PtCl₂, toluene 110 °C for 2 h. ^b 10% PtCl₂, toluene 110 °C for 5 h. ^c 12 h.

for such a reaction.^{13,14} Nevertheless, a detailed picture of the mechanism is still lacking. Indeed, some important questions are yet to be answered, *i.e.*: do the allene substituents affect the reaction mechanism? Are the PtCl₂ and Au(I)-catalyzed processes exhibiting a similar profile? Why do some substrate/catalyst combinations give rise to [4 + 2] instead of [4 + 3] cycloadducts? In order to provide an answer to these questions we present herein a more complete mechanistic study based on computational methods.

Computational details

Calculations were carried out at the DFT (B3LYP) level¹⁵ using the program package Gaussian03.¹⁶ All geometries were fully optimised without any symmetry or geometry constraints. Optimizations were performed with the 6-31G(d) basis set for the main group elements and the Lanl2dz pseudopotential¹⁷ with the associated double- ζ basis set for Pt and Au that includes relativistic effects; an extra series of f-polarization functions were also added for both metal atoms (Pt: exp. = 0.093; Au: exp. = 1.050).¹⁸ The nature of the stationary points was checked by frequency calculations: the minima were confirmed to have no imaginary frequencies, whereas the transition states have only one (saddle points). The solvent effects were computed with the continuum CPCM model by single point calculations on the gas

phase optimised geometries (toluene for PtCl₂ or dichloromethane for gold(I)-complexes); these calculations were done using the same basis set and pseudopotential for Pt and Au but a larger 6-311++G(d,p) basis set for all other atoms. The energies given in the text, G_{solv} , were obtained by adding the thermodynamic corrections from the gas phase frequency calculations (using the 6-31G(d) basis set), to the energy in solution (using the 6-311++G(d,p) basis set) (eqn (1)).¹⁹

$$G_{\text{solv}} = E_{\text{solv}} + (G_{\text{gas}} - E_{\text{gas}}) \quad (1)$$

A topological analysis of the electron density (obtained from Gaussian calculations) was performed to calculate the density (ρ) and the ellipticity (ϵ) for bonds using Bader's atoms in molecules (AIM) theory²⁰ and Xaim 1.0 program.²¹ NBO analysis was computed with the NBO 5.0 program.²²

Results and discussion

The mechanistic study on the allene-diene cycloaddition reaction is presented in two sections. The first one analyzes the reaction mechanism with PtCl₂, while the second is devoted to study the performance of Au(I) catalysts.

General mechanistic scheme for PtCl₂-catalyzed cycloadditions

The theoretical study on the mechanism of the [4C+3C] cycloaddition catalysed by PtCl₂ was first performed by analysing the potential surface of a dimethyl-allene substrate that simulates the experimental precursor **1A**, the only difference relying on the fact that X is CH₂ instead of C(CO₂Et)₂ (Table 1). Fig. 1 shows the energy profile, along with a schematic representation of the intermediates and transition states. Their corresponding 3D structures are depicted in Fig. 2.

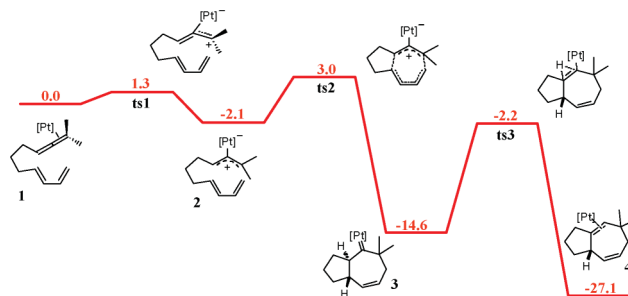


Fig. 1 Gibbs energy profile (in kcal mol⁻¹) for the PtCl₂-catalysed [4C+3C] cycloaddition of a dimethylallene containing substrate (**1a**), [Pt] = PtCl₂.

The reaction begins by coordination of the allene subunit to the catalyst. The initial structure **1** corresponds to a η^2 -coordination involving one of the two C–C double bonds from the allene (this point is selected as the energy reference). Formation of the metal allyl cation intermediate is favourable by –2.1 kcal mol⁻¹; this process takes place very easily with an energy barrier of only 1.3 kcal mol⁻¹ (**ts1**). Intermediate **2** can be depicted as a σ -allylic cation as shown by the coplanarity of the involved carbons and their substituents (both methyls on C₃, Pt atom on C₂, and hydrogen and the first carbon of the organic chain on C₁). All dihedral angles defined taking the three allene carbons and each substituent are between 0° and 8.4°, thus confirming the allylic nature of such a structure.

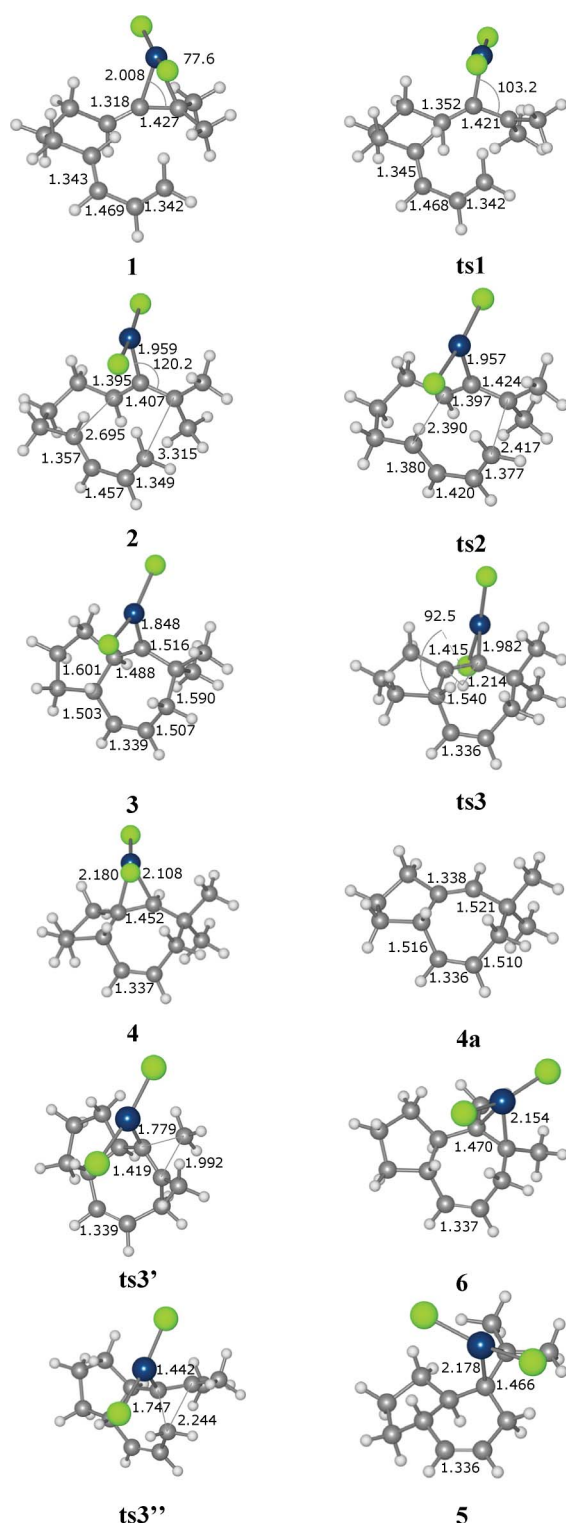


Fig. 2 Structures of intermediates and transition states found for the PtCl_2 -cycloaddition of a dimethylallene substrate model.

Subsequently, this species evolves by an intramolecular concerted $[4\text{C}+3\text{C}]$ cycloaddition. This process can take place *via* an *exo*- or *endo*-like approach, which provides two different diastereoisomers. The observed *exo* selectivity is consistent with the computational results: the *exo*-like approach (**ts2**, 5.1 kcal mol⁻¹) is favoured compared to the *endo*-like (**ts2'**) by

10.0 kcal mol⁻¹ (Fig. 3). The geometry of **ts2** shows that in this case the cycloaddition is a nearly synchronous process (distance of bond forming: $d(\text{C}_1-\text{C}_4) = 2.390 \text{ \AA}$, $d(\text{C}_3-\text{C}_7) = 2.417 \text{ \AA}$). The transformation implies a rearrangement of 6π electrons ($4e+2e$) that forms two single and a new double C–C bond, as a common Diels–Alder reaction.²³ Moreover, the geometry of the resultant heptacyclic species **3** shows that the C_2 –Pt bond is shorter by 0.109 Å than for the previous intermediate **2**. This suggests the presence of a carbene-like unit in which there is an electron back donation from Pt to the carbon. NBO analysis of this intermediate reaffirms this interpretation because of the highly populated σ and $\pi(\text{C}_2-\text{Pt})$ bonds, with $1.814 e^-$ and $1.947 e^-$, respectively. The Mayer bond order is higher than one, 1.3041. Moreover, Bader analysis goes in the same direction with an electron density (ρ) of 0.2056 a.u and an ellipticity value (ϵ) of 0.1283 (see ESI†).²⁴

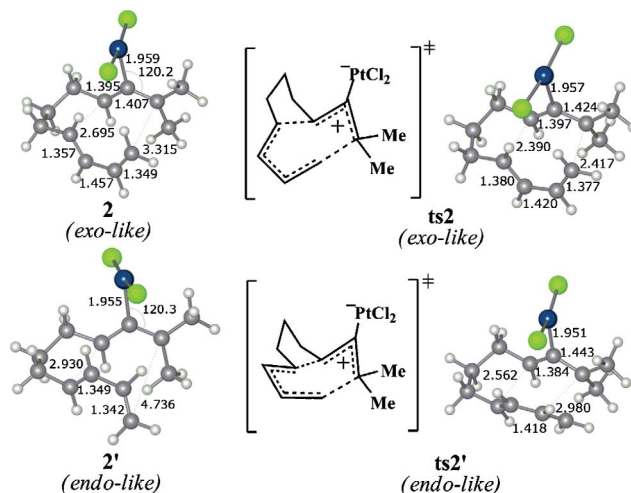
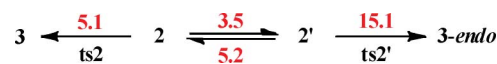


Fig. 3 Structures of metal allyl cation and cycloaddition transition states for the *exo*- and *endo*-like approaches.

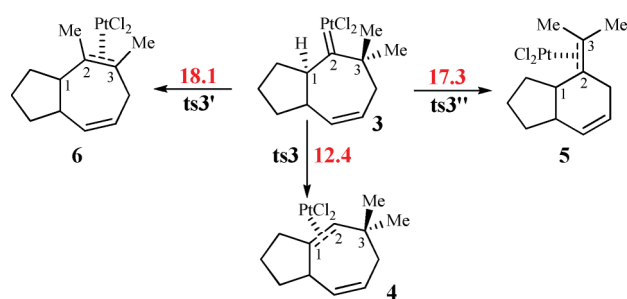
For the *endo*-like approach the **ts2'** geometry suggests an *asynchronous* cycloaddition process (distance of bond forming: $d(\text{C}_1-\text{C}_4) = 2.566 \text{ \AA}$, $d(\text{C}_3-\text{C}_7) = 2.255 \text{ \AA}$). Moreover, structure **2'** (the one arranged for an *endo* attack) can be transformed to intermediate **2** through a low energy pathway with an associated energy barrier of 5.2 kcal mol⁻¹ (Scheme 1). This implies that the *endo*-like **2'** intermediate prefers to revert to **2** instead of undergoing the cycloaddition to **3-endo**.



Scheme 1 Pathways involved in the *exo/endo* selectivity.

Species **3** is the most stable intermediate in the process (−14.6 kcal mol⁻¹), even though the carbenic moiety is expected to be a reactive position. At this stage, 1,2-migrations of any hydrogen or alkyl groups located at the adjacent positions of the carbene (C_1 and C_3) might take place. Therefore, methyl substituents at C_3 or a hydrogen at C_1 , may undergo this 1,2-migration. On the other hand, a ring contraction of the seven-membered cycle to form a six-membered ring is also possible, a process that is in fact a 1,2-alkyl migration.

All of these pathways were computationally investigated (see Scheme 2). The energy barrier for the 1,2-hydrogen migration that



Scheme 2 Evaluated pathways from carbenic intermediate **3** for PtCl_2 catalyst (ΔG^\ddagger in kcal mol^{-1}).

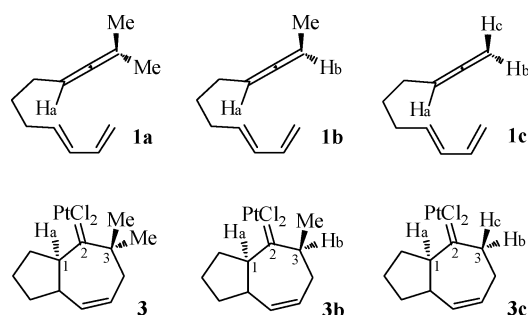
produces the experimentally observed cycloheptene cycloadduct **4a** is of $12.4 \text{ kcal mol}^{-1}$ (**ts3**). 1,2-migration of any of the two methyl groups at C_3 , that generates the heptacyclic product **6**, requires an energy barrier of $18.1 \text{ kcal mol}^{-1}$ (**ts3'**) (Scheme 2). The ring contraction process producing a six-membered cycloadduct (**5**) presents an energy barrier of $17.3 \text{ kcal mol}^{-1}$ (**ts3''**). Although all the possibilities are energetically accessible, the 1,2-hydrogen migration is clearly the most favoured one. These results are in full agreement with the experimental results with **1A**, whose cycloaddition leads to **4A**, the product arising from a 1,2-hydrogen shift.

Any of the 1,2-migration processes generates a new C–C double bond between C_2 and the corresponding α -carbon (C_1 or C_3), simultaneous to the $\sigma(\text{C}_2\text{--Pt})$ bond breaking (Fig. 2, **ts3**, **ts3'** and **ts3''**). The $\text{C}_1\text{--C}_2$ bond distance goes from 1.488 \AA in **3**, to 1.338 \AA in the final product **4a** with a distance of 1.415 \AA in **ts3**; thereby evolving from single to double bond character (Fig. 2). The $\text{C}_2\text{--Pt}$ bond distance, however is enlarged from 1.848 \AA in **3**, to 1.982 \AA in **ts3** and to 2.108 \AA in **4**, indicating the formation of a coordinated $\text{C}_1\text{--C}_2$ double bond to PtCl_2 ($d(\text{C}_1\text{--Pt}) = 2.180 \text{ \AA}$ in **4**, Fig. 2). Moreover, **ts3''** showed a *product like* structure with the heptacycloadduct already broken $d(\text{C}_3\text{--C}_7) = 2.244 \text{ \AA}$, and the new C–C bond closer to be formed $d(\text{C}_2\text{--C}_7) = 1.747 \text{ \AA}$. The theoretical data suggest that the 1,2-hydrogen migration involves a conformational change in intermediate **3**. This change can be followed by the $\text{H}\text{--C}_1\text{--C}_2\text{--Pt}$ dihedral angle value: it changes from 144.1° in **3** to 92.5° in **ts3**. The $\text{C}_1\text{--C}_2$ double bond of the final cycloheptene adduct is η^2 -coordinated to the metal (**4**), therefore closing of the catalytic cycle requires an exchange of the catalyst with the starting allenediene.

To sum up, the formation of the rather stable intermediate **3** is quite accessible as it involves relative energy values of 1.3 and $5.1 \text{ kcal mol}^{-1}$ for **ts1** and **ts2**, respectively. The 1,2-hydrogen migration has the highest energy barrier ($12.4 \text{ kcal mol}^{-1}$, **ts3**), therefore becoming rate-determining.

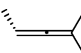
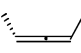
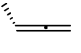
The effect of substituents in the allene

Experimental results show that the reaction outcome is strongly dependent on the number of substituents on the allene moiety. Substrate **1B** gave the cycloheptenyl cycloadduct with a lower yield (62%) than substrate **1A** (92%), whereas the reaction of substrate **1C** fails to give the $[4\text{C}+3\text{C}]$ product, albeit we could isolate a small amount of a $[4\text{C}+2\text{C}]$ cycloadduct (**5C**, 23% yield) (Table 1 entries 1, 2 and 3). This trend was evaluated analysing the potential surface of substrates **1a**, **1b** and **1c** (in the calculated model $\text{X}=\text{CH}_2$, Scheme 3). In principle we assumed a similar



Scheme 3 Structures of substrates **1a**, **1b** and **1c**, and their respective 7-membered intermediates **3**, **3b** and **3c**.

Table 2 Values of the energy barriers and relative metal allyl cation stabilities for the model allenes **s-a**, **s-b** and **s-c** (Gibbs energies in kcal mol^{-1})

Allene models	ts1 (Energy barrier)	Metal allyl cation (Relative energy)
 s-a	2.9	1.6
 s-b	13.1	8.6
 s-c	18.2	12.1

reaction mechanism for all substrates: activation of the allene moiety to give a metal allyl cation intermediate, cycloaddition to a seven-membered ring intermediate, and 1,2-hydrogen migration generating the final product coordinated to the catalyst. However some differences were found depending on the substrate. For instance, for **1b** and **1c** we found that the $[4\text{C}+3\text{C}]$ annulation can take place directly from the initial η^2 -coordinated species. Energy barriers for these direct $[4\text{C}+3\text{C}]$ cycloadditions are $8.4 \text{ kcal mol}^{-1}$ for **1b** and 18.4 for **1c**, respectively. Using substrate **1b** a metal allyl cation intermediate could be located when the diene moiety is far from the allene, in order to disfavour the direct cycloaddition. However the energy barrier to form this intermediate ($16.8 \text{ kcal mol}^{-1}$) makes it less accessible than the direct cycloaddition product.

To further analyse this different behaviour depending on the allene substituents, we measured the stability of allyl cation intermediates derived from a set of model allenes **s-a**, **s-b** and **s-c** (Table 2). The relative energies between the η^2 -coordination and the metal allyl cation species show that the less substituted is the allene, the less stable is the metal allyl cation intermediate (Table 2). The formation of the metal allyl cation from the allene requires 1.6, 8.1 and $12.1 \text{ kcal mol}^{-1}$ for **s-a**, **s-b** and **s-c**, respectively. The energy barriers (**ts1**) for the formation of the corresponding metal allylic cations also show the same trend: 2.9, 13.1 and $18.2 \text{ kcal mol}^{-1}$. These results confirm that the stability of the carbocation generated during the process depends on allene substitution, which is also consistent with the fact that the cycloaddition of **1b** and **1c** are predicted to proceed without the formation of the allyl cations.

These results are also in agreement with the theoretical results for substrate **1d** (model of **1D** with $\text{X}=\text{CH}_2$, Table 1 entry 4). A phenyl group is a π -electron donor substituent that can stabilize the metal allyl cation intermediate better than a methyl group such as

Table 3 Values of the energy barriers for the analyzed [4C+3C] cycloaddition of substrates **1a**, **1b** and **1c** (Gibbs energies in kcal mol⁻¹)

	1a	1b	1c
ts1	1.3	—	—
ts2	5.1	—	—
Direct cycloaddition	—	8.4	18.4
1,2-H_a migration (ts3)	12.4	12.9	11.7
1,2-H_b migration	—	10.2	21.7
1,2-H_c migration	—	—	20.6

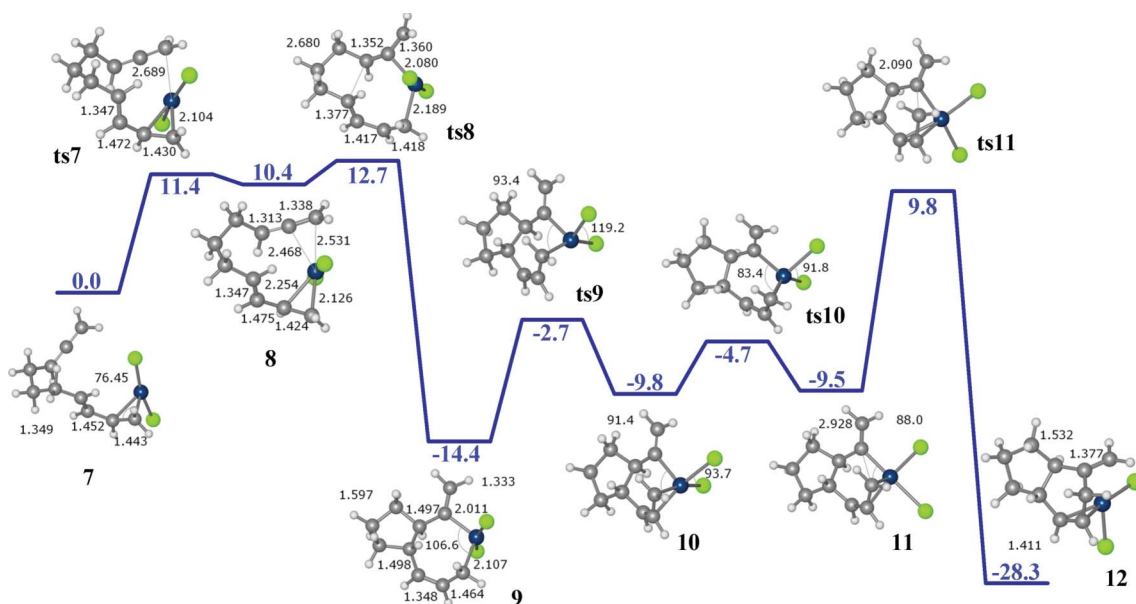
in **1b**. Accordingly, the analysis of the potential energy surface of **1d** showed an accessible metal allyl cation, only 3.3 kcal mol⁻¹ less stable than the η^2 -precursor, with an energy barrier of 4.1 kcal mol⁻¹.

We then studied the 1,2-hydrogen migration on the cycloheptene platinum intermediates **3b** and **3c**, resulting from the cycloaddition of **1b** and **1c**, respectively. We checked the process for all possible migrating α -hydrogens, H_a and H_b for **3b**, and also H_c for **3c** (Scheme 3). 1,2-H_b migration for **3b** is favoured over that of H_a; the corresponding energy barriers are 10.2 kcal mol⁻¹ and 12.9 kcal mol⁻¹, respectively (Table 3). This is in agreement with the selectivity observed in the cycloaddition of **1B** leading to **4B**. On the other hand, **3c** presents a lower energy barrier for the 1,2-H_a migration (11.7 kcal mol⁻¹) than for the other hydrogens H_b and H_c (21.7 and 20.6 kcal mol⁻¹ respectively, Table 3), which suggests that the most favourable 1,2-hydrogen migration might take place from the most substituted adjacent carbon atom. However, as commented previously, the allenediene **1c** does not give rise to any (4 + 3) cycloadduct, but only a (4 + 2) cycloadduct **5C** is obtained in low yield suggesting that alternative reaction pathways might be operating (see below).

Although the formation of this alternative [4C+2C] product could be explained in terms of a ring contraction process, we found that this step is energetically quite demanding (29.6 kcal mol⁻¹), much higher than the alternative 1,2-hydrogen migration

(11.7 kcal mol⁻¹). Therefore it must be an alternative mechanistic pathway with a lower activation barrier that explains the formation of the [4C+2C] cycloaddition product **5C** (Table 1). The potential energy surface for other mechanistic possibilities were then analysed in detail; in particular we considered either a direct (4 + 2) cycloaddition between the allene and diene or a stepwise process. Although we could locate a transition state for a direct (4 + 2) cycloaddition when the C₂–C₃ double bond of the allene is η^2 -coordinated to the catalyst, this pathway has a very high energy barrier, 36.8 kcal mol⁻¹, and hence it can be discarded. On the other hand we found a potential stepwise mechanism that starts with a η^2 -coordination of PtCl₂ to the diene moiety (**7**, Fig. 4). This species is 3.3 kcal mol⁻¹ less stable than that with the coordinated allene (**1**). Then, the system evolves by establishing a bonding interaction between the metal center and the allene moiety, like in **8**. This intermediate easily rearranges in a concerted step to form a new C₁–C₄ bond, and both η^2 -coordinated double bonds become η^1 -alkyl coordinated ligands forming a metallacycle intermediate **9**. The overall energy barrier for this process is 12.7 kcal mol⁻¹. This intermediate **9** can be formally considered a Pt^{IV} species. NBO analysis describes two σ bonds, σ (C₂–Pt) and σ (C₇–Pt) with a population of 1.893 e⁻ and 1.889 e⁻ and a Mayer bond order of 0.9286 and 0.8452, respectively. Bader analysis also identifies both bond critical points with electron densities (ρ) of 0.1458 and 0.1185 u.a for C₂–Pt and C₇–Pt, respectively.

The geometry around the tetracoordinated metal center must change before the system can undergo a reductive elimination step. Indeed, we have found intermediates **10** and **11**, whose formation involves energy barriers of 11.7 and 5.1 kcal mol⁻¹, respectively. The last step generates the C₂–C₇ bond and yields the experimentally observed [4C+2C] product. The oxidative addition step (12.7 kcal mol⁻¹, **ts8**) is more favoured than the alternative [4C+3C] cycloaddition previously commented on (18.4 kcal mol⁻¹), however the energy barrier for the reductive elimination is higher (24.2 kcal mol⁻¹, **ts11**). Importantly, the metallacyclic intermediate **9** is quite stable and once formed it might prefer to evolve to the

**Fig. 4** Gibbs energy profile (in kcal mol⁻¹) of the stepwise mechanism found for substrate **1c** catalysed by PtCl₂.

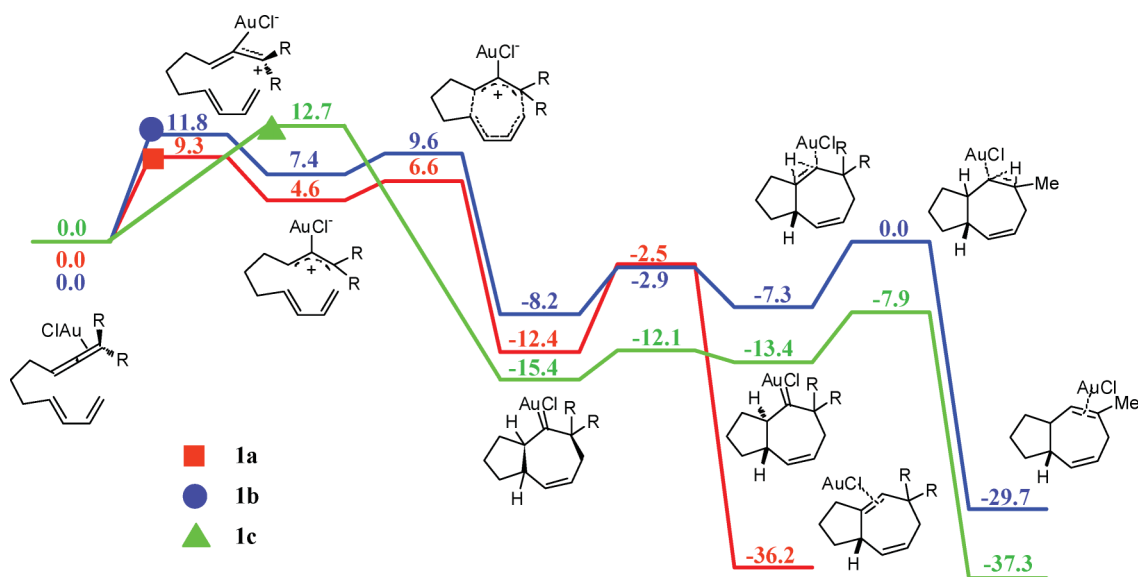


Fig. 5 Gibbs energy profiles (in kcal mol⁻¹) of allene-diene cycloaddition catalysed by AuCl.

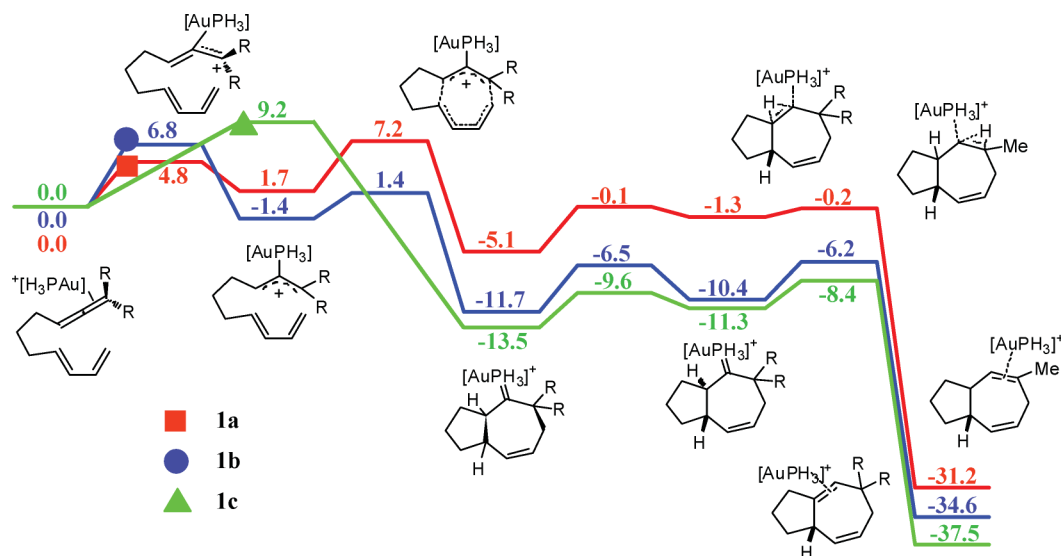


Fig. 6 Gibbs energy profiles (in kcal mol⁻¹) of allene-diene cycloaddition catalysed by [AuPH₃]⁺.

cycloadduct than revert to the starting precursors. Qualitatively, this mechanism is in agreement with the experimental results: no [4C+3C] product is observed, but we did observe the formation of a low yield of the [4C+2C] product. We have also calculated an energy barrier of 30.3 kcal mol⁻¹ for the metal-free [4C+2C] cycloaddition. In agreement with this high barrier, no reaction was experimentally observed without catalyst.

Reaction catalysed by gold(i)-complexes

This section is devoted to the analysis of the intramolecular cycloaddition reaction of allenediene catalysed by gold(i) complexes, in order to compare the results with those obtained for PtCl₂. The first subsection analyses the effect of the allene substituents on the cycloadditions catalysed by AuCl and [AuPH₃]⁺. The second subsection analyses other gold(i) catalysts.

The effect of the allene substituents

Allene-diene cycloaddition reactions of dimethylated, monomethylated and unsubstituted substrates **1a**, **1b** and **1c** (shown in Scheme 3) were analysed using AuCl, and [AuPH₃]⁺ as model catalysts. The energy profiles of the processes are shown in Fig. 5 and Fig. 6. For AuCl the reaction mechanism with the allene precursors **1a** and **1b** follows the standard three steps found for PtCl₂ with **1a**. The energy barrier for the metal allyl cation formation is of 9.3 kcal mol⁻¹ and 11.8 kcal mol⁻¹, respectively. The subsequent [4C+3C] cycloaddition exhibits very low energy barriers for both substrates, 2.0 and 2.2 kcal mol⁻¹, respectively.

For **1c** we found that the cycloaddition occurs in a direct manner, with an energy barrier of 12.7 kcal mol⁻¹. Therefore, as with PtCl₂, the less substituted is the allene, the less accessible is the metal allyl cation intermediate, albeit with PtCl₂ in the case of **1b** we did not observe metal allyl cation intermediates and, with AuCl, we can

detect them. Once the 7-membered ring intermediate is formed, the reaction evolves to the final cycloheptenyl product *via* a 1,2-H migration. The migrating hydrogen depends on the substrate: H_a for **1a** and **1c**, with energy barriers of 9.9 kcal mol⁻¹ and 7.5 kcal mol⁻¹ respectively, and H_b for **1b**, with an energy barrier of 8.2 kcal mol⁻¹ (see Scheme 3). Such migrations take place in a single step for substrate **1a**, whereas for substrates **1b** and **1c** we found that it requires a previous conformational change of the ring, analogous to that observed in the 1,2-hydrogen migration transition state (**ts3**) for PtCl₂.

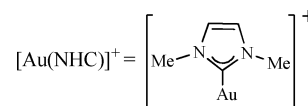
The reaction mechanism for the [AuPH₃]⁺ as a model for a cationic gold catalyst presents a qualitatively similar profile to that for AuCl, although with smaller energy barriers. For instance, the formation of the metal allyl cation intermediate seems to be easier, with energy barriers of 4.8 kcal mol⁻¹ and 6.8 kcal mol⁻¹ for substrates **1a** and **1b**, respectively. The cycloaddition steps, however, are slightly higher in energy: 5.5 kcal mol⁻¹ for **1a** and 2.8 kcal mol⁻¹ for **1b**. For the substrate **1c**, the formation of the seven-membered ring intermediate takes place in a single step with an energy barrier of 9.2 kcal mol⁻¹. With regard to the 1,2-H migration the processes are similar to those found for AuCl, but with slightly smaller energy barriers: 5.0 kcal mol⁻¹ for **1a** (H_a), 5.1 kcal mol⁻¹ for **1c** (H_a) and 5.5 kcal mol⁻¹ for **1b** (H_b), respectively.

Comparison of the results between both gold complexes indicates a similar cycloaddition mechanistic profile. Both catalysts present a less stable metal allyl cation intermediate for **1b** than **1a**, whereas for **1c** we located a direct cycloaddition from the η²-coordination with a higher energy barrier than those of the cycloadditions of **1a** and **1b** (Fig. 5 and 6). On the other hand, AuCl presents higher energy barriers for metal allyl cation formation and the 1,2-hydrogen migration.²⁵

The experimental results with AuCl and PPh₃AuCl/AgSbF₆ are qualitatively consistent with these theoretical data. AuCl induced a clean cycloaddition reaction of substituted allenediene **1a** to give the expected cycloheptenyl product (79% yield of **4a** after 2 h at rt).¹³ Curiously, PPh₃AuCl/AgSbF₆ provided a 80% global yield of a 7 : 3 mixture of cyclohexenyl and cycloheptenyl cycloadducts **5a** and **4a** (*vide infra*).^{26,14} In contrast to the case of PtCl₂, unsubstituted allenediene **1c** did not react either with AuCl or with [AuPPh₃Cl/AgSbF₆] at room temperature (recovery of the starting materials after 12 h),²⁷ whereas **1b** only reacted with [AuPPh₃Cl/AgSbF₆], anyhow to provide a complex mixture of products that includes the (4 + 3) cycloheptenyl product **4b** (50% conversion after 12 h).²⁸

Mechanism for the reaction of cationic gold(i) complexes with dimethylallenyl precursor **1a**

Experimentally it was observed that the catalyst [(IPr)AuCl/AgSbF₆] leads to a faster and cleaner [4C+3C] cycloaddition of **1a** than AuCl or [AuPPh₃Cl/AgSbF₆].¹³ The potential energy surface for the reaction of **1a** was theoretically analysed using a [Au(NHC)]⁺ complex (Scheme 4) as a model of [(IPr)Au]⁺ (a σ-electron-donating ligand). The reaction mechanism is qualitatively similar to that previously discussed for the other gold(i) catalysts: (i) formation of a metal allyl cation, (ii) [4C+3C] cycloaddition to give a gold carbene-like species and (iii) 1,2-hydrogen migration. The relative energy barrier for the metal allyl formation is 5.2 kcal mol⁻¹, whereas that of the [4C+3C]



Scheme 4 Structure of model catalyst [Au(NHC)]⁺.

cycloaddition is 6.2 kcal mol⁻¹. Interestingly, the 1,2-hydrogen migration presents a lowest relative energy barrier (5.0 kcal mol⁻¹) than that observed in previous cases, which might justify the experimental observation of a faster reaction.¹³

We have also analysed the potential energy surface for the reaction of **1a** in the presence of [AuP(OMe)₃]⁺ (model of [AuP(OAr)₃]⁺). It has been experimentally observed that the reaction of **1a** catalysed by [(ArO)₃PAu⁺SbF₆⁻; Ar = 2,4-di-*tert*-butylphenyl]) gives a 72% yield of [4C+2C]/[4C+3C] products **4a** and **5a** in a 10 : 1 ratio.¹⁴ The reaction mechanism for the formation of the [4C+3C] cycloaddition product **4a** follows the standard allene activation-cycloaddition-1,2-H migration mechanism (Fig. 7). The formation of the [4C+2C] product **5a** might be explained by three different mechanisms: (i) a mechanism starting by a concerted [4C+3C] cycloaddition followed by ring contraction instead of a 1,2-hydrogen migration; (ii) a concerted [4C+2C] cycloaddition catalysed by the gold complex; (iii) a stepwise mechanism involving a metallacycle intermediate.

The energy profiles of these mechanisms are shown in Fig. 7. The energy barrier for the [4C+3C] cycloaddition is 6.4 kcal mol⁻¹ (**ts2-PO**; PO indicates phosphite-gold catalyst), therefore this pathway is clearly favoured over the others (red profile in Fig. 7). Intermediate **3-PO** may evolve to form the [4C+2C] product (**5a**) *via* ring contraction (**ts3'-PO**) or the [4C+3C] product (**4a**) *via* 1,2-H-migration (**ts3-PO**). Energy barriers for these two processes are quite similar (7.2 kcal mol⁻¹ and 7.4 kcal mol⁻¹). If one considers only electronic energy the difference is more marked (1.6 kcal mol⁻¹). Therefore, the tendency is consistent with the experimental observation of the cyclohexene **5a** as the major reaction product.^{29,13,14} Moreover, **ts3'-PO** showed that the ring contraction process is less advanced in the transition state (d(C₁-C₇) = 2.033 Å, d(C₂-C₇) = 1.908 Å) compared with PtCl₂ (**ts3'**), having a more *reactant*-like transition state (Fig. 8).

The proposed mechanistic divergence from the seven-membered ring gold carbene intermediate **3-PO** is also in agreement with experimental findings which indicate that the [4C+2C] and [4C+3C] cycloadducts **4a** and **5a** are always obtained with the same enantiomeric excess when chiral phosphoramidite-gold(i) complexes are used as catalysts.^{14,30}

A concerted [4C+2C] Diels–Alder type of reaction presents an energy barrier of 14.3 kcal mol⁻¹ (green),³¹ and the energy barrier for a step-wise mechanism *via* metallacyclic species is of 15.8 kcal mol⁻¹ (blue), both clearly higher in energy than that of the [4C+3C]/ring contraction process (red), which is therefore the most probable mechanistic pathway for these allenediene cycloadditions catalysed by [(ArO)₃PAu]⁺SbF₆⁻.

The [4C+2C] cycloaddition step is a concerted and asynchronous process (**ts7-PO**, distance of bond forming: d(C₁-C₄) = 1.918 Å, d(C₂-C₇) = 3.586 Å) that evolves from the intermediate **7-PO** (Fig. 8). This species can be described as an η¹-coordinated bent allene²⁵ that is formed easily with an energy barrier of 3.0 kcal mol⁻¹ (**ts6-PO**) from the initial η²-coordinated allene **6-PO**.

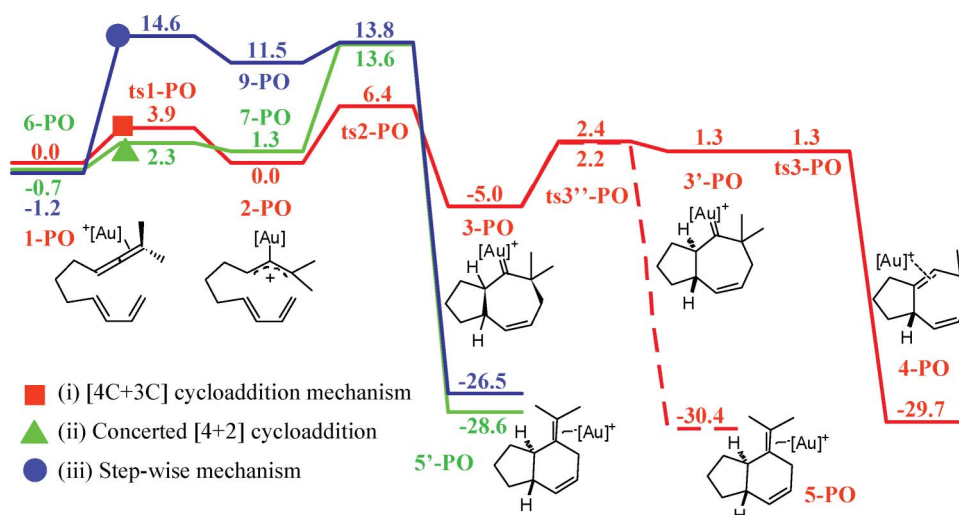


Fig. 7 Gibbs energy profiles (in kcal mol⁻¹) of different evaluated cycloaddition mechanisms of **1a** using [AuP(OMe)₃]⁺ as a model catalyst.

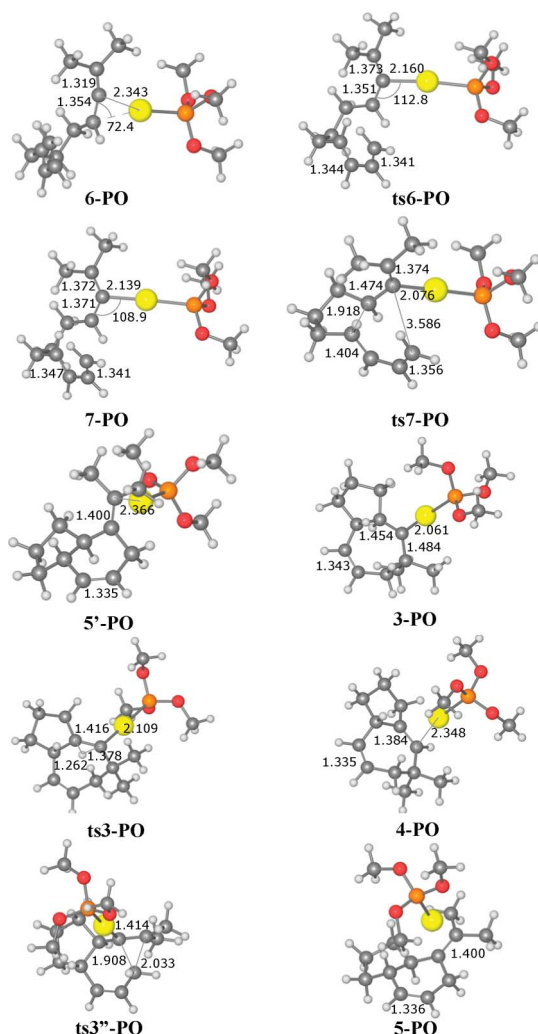


Fig. 8 Structures of selected intermediates and transition states found using [AuP(OMe)₃]⁺ as a model catalyst.

Interestingly, the stepwise mechanism shows a formal metallacycle, intermediate **9-PO**, that can be related to intermediate

9 found for the reaction of **1c** catalysed by PtCl₂ (see Fig. 4). However, when compared to the reactants the Pt-metallacycle is more stable by 14.4 kcal mol⁻¹, whereas that of Au is unstable by 11.5 kcal mol⁻¹ (Fig. 4 and Fig. 7, respectively). The metallacyclic structures **9** and **9-PO** are shown in Fig. 9.

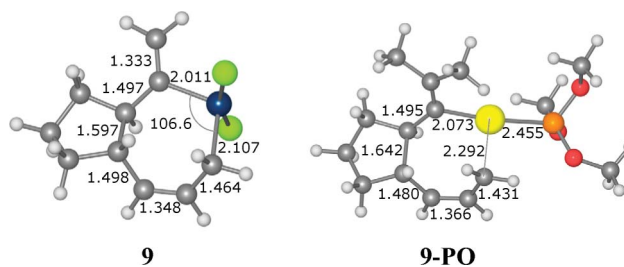


Fig. 9 Structures for Pt- and Au-intermediates **9** and **9-PO**.

The geometry of both structures shows that the M–C distances are longer for Au, especially with the carbon atom coming from the diene ($d(\text{Pt}-\text{C}_7) = 2.107 \text{ \AA}$, $d(\text{Au}-\text{C}_7) = 2.292 \text{ \AA}$). NBO and Bader analysis describes a formal Pt^{IV}-metallacycle with two $\sigma(\text{C}-\text{Pt})$ bonds (*vide supra*). Different results are obtained when analysing the formal Au-metallacycle. NBO analysis does not identify a $\sigma(\text{C}-\text{Au})$ bond, it shows an empty $p\pi$ -orbital on C₇, partially accepting electrons from the Au center. Bader analysis localizes a bond critical point along the C₇–Au path with a rather low electron density (ρ) of 0.0758 a.u. It is clearly lower than that found for C₂–Au ($\rho = 0.1268 \text{ a.u.}$), and that in the case of PtCl₂ (intermediate **9**, C₇–Pt) with an electron density (ρ) of 0.1185 a.u., suggesting a major ionic bond character in **9-PO**. Related gold metallacycles were recently proposed by Toste and co-workers in the context of the gold(I) catalysed intramolecular [2C+2C] cycloadditions of allenenes.^{6h}

The above data indicate that the cycloheptenyl carbene intermediates are therefore common for the formation of cycloheptenyl ([4C+3C]) or cyclohexenyl ([4C+2C]) products (Fig. 7). According to the experimental results, PtCl₂ and [Au(NHC)]⁺ show a quite clear preference for the 1,2-H shift process, whereas for [AuP(OMe)₃]⁺ the 1,2-alkyl shift (ring contraction) becomes more

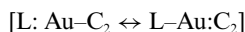
Table 4 Gibbs energy barriers of the 1,2-hydrogen migration and ring contraction pathways

Catalyst	1,2-H migration ts3	1,2-ring contraction ts3''
PtCl ₂	12.4	17.3
AuCl	9.9	13.1
[AuPH ₃] ⁺	5.0	7.6
[AuP(OMe) ₃] ⁺	7.4	7.2
[Au(NHC)] ⁺	5.0	9.7

favoured than the 1,2-H migration. We have already compared the 1,2-hydrogen migration and ring contraction pathways in the case of PtCl₂ and [AuP(OMe)₃]⁺ catalysts for substrate **1a**. For the sake of completeness, the analogous pathways for [Au(NHC)]⁺, AuCl and [AuPH₃]⁺ catalysts were also computed. The relative energy barriers for these two processes are shown in Table 4. The theoretical values are consistent with the experimental findings showing that the hydrogen migration is clearly favoured in all the cases except the P-ligands. For the latter ligands a mixture of products is predicted, with the [AuP(OMe)₃]⁺ favouring the 1,2-alkyl shift. Moreover, the PtCl₂ catalyst shows the highest relative energy barriers for both processes (1,2-hydrogen migration and ring contraction). This fact can be directly related to the high stability presented by the seven-membered ring carbene intermediate in the energy reaction profile for this catalyst and is consistent with the higher temperature required in these PtCl₂-catalysed [4C+3C] cycloadditions.^{12,13}

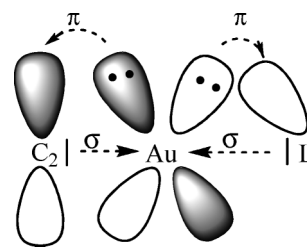
Also significantly, the barrier for the 1,2-H migration with [Au(NHC)]⁺ is only 5.0 kcal mol⁻¹, 4.7 kcal mol⁻¹ lower than that of the ring contraction process, and more than 2 kcal mol⁻¹ lower than that of the 1,2-H migration with [AuP(OMe)₃]⁺, confirming the preference of catalysts with this type of ligands to give [4C+3C] cycloadducts (Table 4).

The nature of the M–C bond in the seven-membered ring intermediates of type **3** depends on the metal and ancillary ligands used. For the case of Pt there is a near double occupancy of the σ(C–Pt) and π(C–Pt) orbitals. Gold intermediates, however, show a σ(C–Au) orbital along with an empty orbital on C₂ (pπ-orbital) with an important π-electron backdonation from an occupied d-orbital of the metal, whose strength depends on the ligand attached to the gold atom (see ESI†). Moreover, when considering the L–Au–C₂ fragment the description is less simple: this is mainly due to fact that there is only one empty orbital on gold (6 s) forcing a three-centre-four-electron σ-hyperbond.^{32,33}



NBO analysis shows a preference for the [L: Au–C₂] hyperbond structure along with a high electron donation from the lone pair of the L ligand to the σ*(C–Au). Thus, the C–M bond order depends on the π-backdonation from the d-orbital metal to the empty orbital on C₂, and on the σ-donation from the L ligand to the metal. The first interaction increases the C–M bond order, whereas the second one has the opposite effect. A much less important backdonation from a Au d-orbital to the L ligand was also observed, mainly for the L = POR₃ ligand. All of these interactions have been schematically represented in Fig. 10.

Thus, the electronic distribution on the C₂–Au–L fragment is affected by the nature of the L ligand. The Cl[–] ligand, giving rise to a neutral complex, is the most electronegative and also

**Fig. 10** Schematic representation of the bonding interactions at the C₂–Au–L fragment.

a π-donating ligand therefore allowing the major backdonation from the d metal orbital to the C₂ pπ-orbital: the donor–acceptor interaction energy is calculated by NBO second order perturbation theory analysis to be 30.5 kcal mol⁻¹. This interaction energy for NHC, PH₃ and P(OMe)₃ ligands is reduced to 18.2, 15.2 and 15.1 kcal mol⁻¹, respectively. A classification of all the analysed metal complexes, considering the metal-to-C₂ backdonating capacities can be defined as: PtCl₂ > AuCl > [Au(NHC)]⁺ > [AuPH₃]⁺ > [AuP(OMe)₃]⁺. This trend is also observed on other analysed parameters: Mayer bond order, ellipticity and density, and inversely of the observed C–M bond distance (see ESI†).

According to this data, C₂–PtCl₂, C₂–AuCl, or C₂–Au(NHC) species should exhibit a more typical carbene reactivity (where 1,2-H migrations are usually preferred), whereas the reactivity of C₂–AuP(OR)₃ species could be closer to that of a carbocation. Indeed, these species can be understood as gold-coordinated carbocations.

As previously commented, the stability of the seven-membered ring carbene intermediate can be related to the metal electron back donation capacity that in turn, depends on the nature of the ligand. On the other hand, the different backdonation capacity of each metal induces a different electron demand of the C₂ atom over the bicyclic organic unit that it belongs to. The orbital analysis shows an electron donation from the σ(C–H) or the σ(C–C) orbitals to the unoccupied C₂ (pπ-orbital) depending on the conformation of the seven membered ring which results from the [4C+3C] cycloaddition (see ESI†), a conformation that eventually depends on the catalyst used for the cycloaddition. In the reactions with PtCl₂, AuCl or [Au(NHC)]⁺, where the 1,2-hydrogen migration is clearly favoured, the carbene intermediate resulting from the [4 + 3] cycloaddition evolves to favour a conformation in which there is an interaction with the σ(C–H) orbital, to allow the subsequent 1,2-H shift. The electron donation from the σ(C–H) orbitals is reflected on the longer distances obtained when those interactions are taking place.³⁴

An analogous orbital interaction can also take place between the unoccupied C₂ (pπ-orbital) and the σ(C₃–C₇) and σ(C₁–C₄) orbitals. Those interactions are guiding the reaction for the case of [AuP(OMe)₃]⁺, the catalyst for which the C₂ pπ-orbital is more empty, which favours the 1,2-alkyl contraction and, eventually, the formation of the cyclohexene cycloadduct.

Conclusions

The computational analysis of the reaction mechanism for the allene-diene [4C+3C] cycloaddition catalysed by Pt(II) or Au(I) complexes shows that the reaction consists of three main steps: (i) formation of a metal allyl cation intermediate, (ii) cycloaddition

forming a 7-membered ring and (iii) 1,2-hydrogen migration to form the final product. In spite of this, the specific operative reaction mechanism depends on the substrate (*i.e.* the number of substituents in the allene moiety) and the nature of the ligand at the catalyst.

The formation of the initial metal allyl cation strongly depends on the substituents of the allene. For **1a** (double substituted allene) its formation is clearly favoured, and seems to be quite independent of the catalyst. Substrate **1b** (single substituted) forms such an intermediate for Au(I) catalysts but not for PtCl₂, whereas substrate **1c** (no substituents) prefers to evolve directly to the [4C+3C] gold-cycloheptene intermediate.

Energy barriers for the second, [4C+3C] cycloaddition step, range from 2.0 to 6.4 kcal mol⁻¹. These energies are related to the relative stability of the previous metal allyl cation intermediate. The more substituted is the allene the more accessible is the [4C+3C] cycloaddition. Overall, the facility for the formation of the [4C+3C] metal carbene intermediate (combination of the energy barriers for steps (i) and (ii)) can be ranked as follows: PtCl₂ > [AuPOMe₃]⁺ > [AuPH₃]⁺ > AuCl > [Au(NHC)]⁺.

In the case of the dimethylallene precursor **1a** seven-membered ring intermediate may evolve by a 1,2-H migration or by a ring contraction (1,2-alkyl migration). The first process is generally the most favourable one. The energy barrier for such a process is higher for PtCl₂ than for the Au(I) species. The relative energy barrier for the ring contraction, in turn, follows the same trend as the catalyst backdonation capacity: PtCl₂ > AuCl > [Au(NHC)]⁺ > [AuPH₃]⁺ > [AuP(OMe)₃]⁺.

The chemoselectivity between the [4 + 3] and [4 + 2] products can be selected by modifying the ligand at Au(I)-catalysts. The ring contraction pathway is clearly disfavoured over the 1,2-hydrogen migration for PtCl₂. The Au(I) catalysts also favour the 1,2-hydrogen migration over the ring contraction except for a catalyst with a strong π -electron acceptor ligand, such as triarylphosphite. The interaction between the σ (C–H) or σ (C–C) orbitals with the unoccupied $p\pi$ -orbital of the C atom bonded to the metal is shown to guide the reaction.

A different reaction mechanism, a stepwise mechanism, is proposed for the formation of the [4 + 2] cycloadduct product from **1c** (no substituents) using PtCl₂ as a catalyst. For this reaction we have identified an intermediate described as a formal Pt^{IV} metallacycle. In the case of substrate **1a** with the [AuP(OMe)₃]⁺ catalyst, a similar metallacycle intermediate was found. Nevertheless, the formal charge on the Au(I) center remains unchanged.

According to these results, PtCl₂ is the best catalyst for the [4C+3C] cycloaddition itself, however, it is the worst for the 1,2-hydrogen migration (usually, the rate-determining step). Thus, considering the overall reaction mechanism, gold(I) complexes are better catalysts than PtCl₂, and the cationic ones, better than the neutral AuCl. Our results suggest that some computed species might be experimentally accessible depending on the reaction conditions. These studies are now underway in our laboratories.

Acknowledgements

We thank the Spanish MICINN [SAF2010-20822-C02, CTQ2007-67411/BQU, CTQ2008-06866-C02-01, Consolider-Ingenio 2010 (CSD2007-00006) and for a studentship to S-M (FPU)], CSIC and Xunta de Galicia (GRC2010/12, INCITE09 209 122 PR), as

well as the ERDF. The use of the computational facilities of the CESCA is greatly appreciated.

Notes and references

- 1 S. Kobayashi and K. A. Jørgensen, *Cycloaddition Reactions in Organic Synthesis*, Wiley-VCH, Weinheim, 2002.
- 2 M. A. Battiste, M. P. Pelphrey and L. D. Wright, *Chem.–Eur. J.*, 2006, **12**, 3438.
- 3 (a) M. Harmata, *Acc. Chem. Res.*, 2001, **34**, 595; (b) M. Harmata, *Chem. Commun.*, 2010, **46**, 8886; (c) M. Harmata, *Chem. Commun.*, 2010, **46**, 8904.
- 4 For reviews on Pt and Au catalysis using unsaturated systems, see: (a) L. Zhang, J. Sun and S. A. Kozmin, *Adv. Synth. Catal.*, 2006, **348**, 2271; (b) A. Fürstner and P. W. Davies, *Angew. Chem., Int. Ed.*, 2007, **46**, 3410; (c) A. S. K. Hashmi and G. J. Hutchings, *Angew. Chem., Int. Ed.*, 2006, **45**, 7896; (d) A. S. K. Hashmi, *Chem. Rev.*, 2007, **107**, 3180; (e) E. Jiménez-Núñez and A. M. Echavarren, *Chem. Commun.*, 2007, 333; (f) Z. Li, C. Brouwer and C. He, *Chem. Rev.*, 2008, **108**, 3239; (g) H. C. Shen, *Tetrahedron*, 2008, **64**, 3885.
- 5 (a) E. Jiménez-Núñez and A. Echavarren, *Chem. Rev.*, 2008, **108**, 3326; (b) A. S. K. Hashmi, *Angew. Chem., Int. Ed.*, 2010, **49**, 5232; (c) A. S. K. Hashmi, A. M. Schuster, S. Litters, F. Rominger and M. Pernpointner, *Chem.–Eur. J.*, 2011, **17**, 5661; (d) M. Lein, M. Rudolph, A. S. K. Hashmi and P. Schwerdtfeger, *Organometallics*, 2010, **29**, 2206.
- 6 Recent examples of mechanistic studies on Gold(I)-catalyzed reactions involving multiple C–C bonds: (a) G. Kovács, A. Lledós and G. Ujaque, *Organometallics*, 2010, **29**, 3252; (b) G. Kovács, A. Lledós and G. Ujaque, *Organometallics*, 2010, **29**, 5919; (c) P. Pérez-Galán, E. Herrero-Gómez, D. T. Hog, H. J. A. Martin, F. Maseras and A. M. Echavarren, *Chem. Sci.*, 2011, **2**, 141; (d) S. Labouille, A. Escalle-Lewis, Y. Jean, N. Mézailles and P. Le Floch, *Chem.–Eur. J.*, 2011, **17**, 2256; (e) G. Wang, Y. Zou, Z. Li, Q. Wang and A. Goeke, *Adv. Synth. Catal.*, 2011, **353**, 550; (f) P. Nun, S. Gaillard, A. Poater, L. Cavallo and S. P. Nolan, *Org. Biomol. Chem.*, 2011, **9**, 101; (g) M.-Z. Wang, C.-Y. Zhou, Z. Guo, E. L.-M. Wong, M.-K. Wong and C.-M. Che, *Chem.–Asian J.*, 2011, **6**, 812; (h) A. Z. González, D. Benitez, E. Tkatchouk, W. A. Goddard III and F. D. Toste, *J. Am. Chem. Soc.*, 2011, **133**, 5500; (i) M. Pernpointner and A. S. K. Hashmi, *J. Chem. Theory Comput.*, 2009, **5**, 2717.
- 7 For a review of theoretical studies on gold catalyzed cycloadditions involving allenes see: S. Montserrat, G. Ujaque, F. López, J. L. Mascareñas and A. Lledós, *Top. Curr. Chem.*, 2011, **302**, 225.
- 8 H. Funami, H. Kusama and N. Iwasawa, *Angew. Chem., Int. Ed.*, 2007, **46**, 909.
- 9 (a) J. Hee and F. D. Toste, *Angew. Chem., Int. Ed.*, 2007, **46**, 912 For a related paper, see also: (b) X. D. Shi, D. J. Gorin and F. D. Toste, *J. Am. Chem. Soc.*, 2005, **127**, 5802.
- 10 For a review on the use of allenes as three-carbon units in catalytic cycloadditions see: F. López and J. L. Mascareñas, *Chem.–Eur. J.*, 2011, **17**, 418.
- 11 For a recent review on transition-metal cyclizations of allenes, see: (a) C. Aubert, L. Fensterbank, P. García, M. Malacria and A. Simonneau, *Chem. Rev.*, 2011, **111**, 1954 For a recent review on gold-catalyzed cyclizations of allenes see: (b) N. Krause and C. Winter, *Chem. Rev.*, 2011, **111**, 1994.
- 12 B. Trillo, F. López, M. Gullías, L. Castedo and J. L. Mascareñas, *Angew. Chem., Int. Ed.*, 2008, **47**, 951; Recent developments in gold-catalyzed cycloaddition reactions; F. López and J. L. Mascareñas Beilstein, *J. Org. Chem.*, 2011, **7**, 1075–1094.
- 13 B. Trillo, F. López, S. Montserrat, G. Ujaque, L. Castedo, A. Lledós and J. L. Mascareñas, *Chem.–Eur. J.*, 2009, **15**, 3336.
- 14 I. Alonso, B. Trillo, F. López, S. Montserrat, G. Ujaque, L. Castedo, A. Lledós and J. L. Mascareñas, *J. Am. Chem. Soc.*, 2009, **131**, 13020.
- 15 C. Lee, R. G. Parr and W. Yang, *Phys. Rev. B*, 1988, **37**, B785; A. D. Becke, *J. Chem. Phys.*, 1993, **98**, 5648; P. J. Stephens, F. J. Devlin, C. F. Chabalowski and M. J. Frisch, *J. Phys. Chem.*, 1994, **98**, 11623.
- 16 M. J. Frisch, G. W. Trucks, H. B. Schlegel, G. E. Scuseria, M. A. Robb, J. R. Cheeseman, J. A. Montgomery Jr., T. Vreven, K. N. Kudin, J. C. Burant, J. M. Millam, S. S. Iyengar, J. Tomasi, V. Barone, B. Mennucci, M. Cossi, G. Scalmani, N. Rega, G. A. Petersson, H. Nakatsuji, M. Hada, M. Ehara, K. Toyota, R. Fukuda, J. Hasegawa, M. Ishida, T. Nakajima, Y. Honda, O. Kitao, H. Nakai, M. Klene, X. Li, J. E. Knox, H. P. Hratchian, J. B. Cross, V. Bakken, C. Adamo, J. Jaramillo,

- R. Gomperts, R. E. Stratmann, O. Yazyev, A. J. Austin, R. Cammi, C. Pomelli, J. W. Ochterski, P. Y. Ayala, K. Morokuma, G. A. Voth, P. Salvador, J. J. Dannenberg, V. G. Zakrzewski, S. Dapprich, A. D. Daniels, M. C. Strain, O. Farkas, D. K. Malick, A. D. Rabuck, K. Raghavachari, J. B. Foresman, J. V. Ortiz, Q. Cui, A. G. Baboul, S. Clifford, J. Cioslowski, B. B. Stefanov, G. Liu, A. Liashenko, P. Piskorz, I. Komaromi, R. L. Martin, D. J. Fox, T. Keith, M. A. Al-Laham, C. Y. Peng, A. Nanayakkara, M. Challacombe, P. M. W. Gill, B. Johnson, W. Chen, M. W. Wong, C. Gonzalez and J. A. Pople, *Gaussian 03, Revision E.01*, Gaussian, Inc., Wallingford CT, 2004.
- 17 P. J. Hay and W. R. Wadt, *J. Chem. Phys.*, 1985, **82**, 299; W. R. Wadt and P. J. Hay, *J. Chem. Phys.*, 1985, **82**, 284.
- 18 A. Höllwarth, M. Böhme, S. Dapprich, A. W. Ehlers, A. Gobbi, V. Jonas, K. F. Köhler, R. Stegman, A. Veldkamp and G. Frenking, *Chem. Phys. Lett.*, 1993, **208**, 237.
- 19 A. A. C. Braga, G. Ujaque and F. Maseras, *Organometallics*, 2006, **25**, 3647 G_{gas} and E_{gas} calculated using 6-31G(d) basis set.
- 20 R. F. W. Bader, *Atoms in Molecules, a Quantum Theory*, Oxford Science Publication/Clarendon Press, London, 1990; RFW Bader, *Chem. Rev.*, 1991, **91**, 893.
- 21 C. Bo and J. C. Ortiz, *Xaim 1.0*, Universitat Rovira i Virgili, Tarragona, 1998.
- 22 E. D. Glendening, J. K. Badenhoop, A. E. Reed, J. E. Carpenter, J. A. Bohmann, C. M. Morales and F. Weinhold, *NBO 5.0*. Theoretical Chemistry Institute, University of Wisconsin, Madison, 2001.
- 23 For additional theoretical analysis on the [4C+3C] cycloaddition transition state including aromaticity terms, see: I. Fernández, F. P. Cossío Abel de Cózar, A. Lledós and J. L. Mascareñas, *Chem.-Eur. J.*, 2010, **16**, 12147.
- 24 Ellipticity value for ethene double bond is 0.23. See ref. 20.
- 25 V. Gandon, G. Lemièrre, A. Hours, L. Fensterbank and M. Malacria, *Angew. Chem., Int. Ed.*, 2008, **47**, 7534.
- 26 See also: P. Mauleón, R. M. Zeldin, A. Z. González and F. D. Toste, *J. Am. Chem. Soc.*, 2009, **131**, 6348.
- 27 Upon heating, no reaction was observed with AuCl whereas a complex mixture of products was detected with [AuPPh₃Cl/AgSbF₆].
- 28 A yield of the (4 + 3) cycloadduct could not be obtained from this reaction since its purification from the complex crude mixture is complicated by the presence of several side products of similar polarity.
- 29 It is important to remind that additional electronic and steric factors existing in the real catalyst might not be taken into account in these theoretical studies carried out with more simple [AuP(OMe)₃]⁺ and [Au(NHC)]⁺ catalysts.
- 30 See also: D. Benitez, E. Tkatchouk, A. Z. González, W. A. Goddard III and D. Toste, *Org. Lett.*, 2009, **11**, 4798.
- 31 In the reaction energy profile appears an intermediate just before the formation of the [4 + 2] cycloadduct. This intermediate can be described as an η^1 -coordinated bent allene; see Ref. 25.
- 32 C. R. Landis and F. Weinhold, *J. Comput. Chem.*, 2007, **28**, 198.
- 33 D. Benitez, N. D. Shapiro, E. Tkatchouk, Y. Wang, W. A. Goddard III and F. D. Toste, *Nat. Chem.*, 2009, **1**, 482.
- 34 The d(C₁-H) on the seven-membered ring using [Au(NHC)]⁺ catalyst is elongated from 1.091 to 1.115 Å in a conformation that allows the interaction between σ (C₁-H) and C₂ $p\pi$ -orbital.